

**Supplemental Material for**  
**Telecom-band quantum memory with chlorine defects in silicon**  
**carbide**

A. N. Anisimov<sup>1</sup>, K. Mavridou<sup>1</sup>, A. V. Mathews<sup>1,2</sup>, M. Helm<sup>1,2</sup>, and G. V. Astakhov<sup>1</sup>

<sup>1</sup>*Helmholtz-Zentrum Dresden-Rossendorf,*

*Institute of Ion Beam Physics and Materials Research, 01328 Dresden, Germany*

<sup>2</sup>*Technische Universität Dresden, 01062 Dresden, Germany*

## Contents

<b>Supplementary Figures</b>	3
Supplementary Figure S1: Room-temperature time-resolved spectroscopy	3
Supplementary Figure S2: RF-assisted spectroscopy	4
Supplementary Figure S3: RF-induced PL dynamics	5
Supplementary Figure S4: Ramsey fringes	6
Supplementary Figure S5: Experimental geometry	7
<b>Supplementary Text</b>	7
Supplementary Text S1: Simulation of the ODMR spectra	7
<b>Supplementary Tables</b>	9
Supplementary Table S1: Spin state decomposition	9

## SUPPLEMENTARY FIGURES

### Supplementary Figure S1: Room-temperature time-resolved spectroscopy

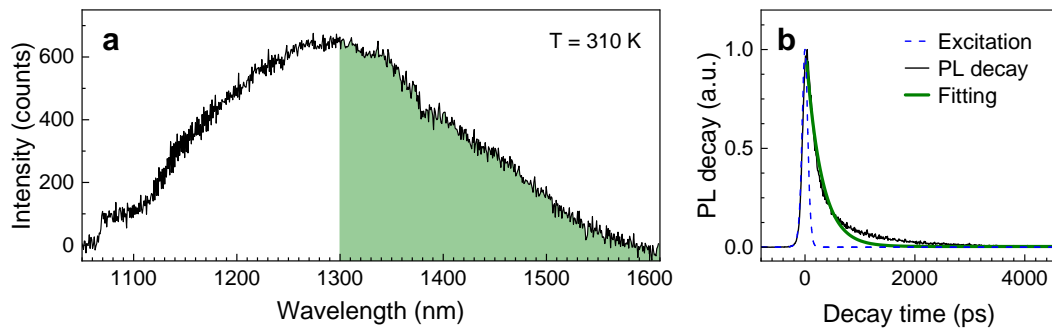


Fig. S1: (a) Room-temperature ( $T = 310\text{ K}$ ) PL spectrum of a  $^{35}\text{Cl}$ -implanted 4H-SiC wafer (sample #1) under optical excitation at  $\lambda_{\text{ex}} = 976\text{ nm}$ . The shaded area indicates the spectral range used for the PL decay measurements, selected with a longpass filter 1300 nm. (b) PL decay measurement under pulsed excitation at  $\lambda_{\text{ex}} = 1060\text{ nm}$  and a pulse duration of 10 ps (the dashed line). The fitting curve represents a convolution of the laser pulse profile and a mono-exponential decay with a time constant of 265 ps.

## Supplementary Figure S2: RF-assisted spectroscopy

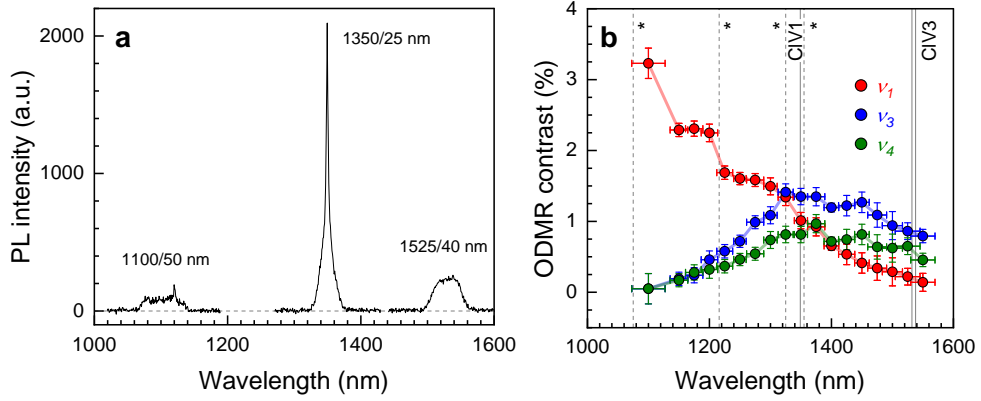


Fig. S2: (a) PL spectra measured with different bandpass filters from sample #1 under optical excitation at  $\lambda_{\text{ex}} = 976$  nm and at temperature  $T = 10$  K. (b) ODMR contrast for the  $\nu_1$ ,  $\nu_2$  and  $\nu_3$  resonances detected with different bandpass filters. The vertical solid lines corresponds to the CIV1 and CIV3 ZPL. The vertical dashed lines correspond to ZPLs labeled with asterisks (\*) in the main text. The vertical error bars represent standard deviation. The horizontal error bars represent the spectral detection windows.

### Supplementary Figure S3: RF-induced PL dynamics

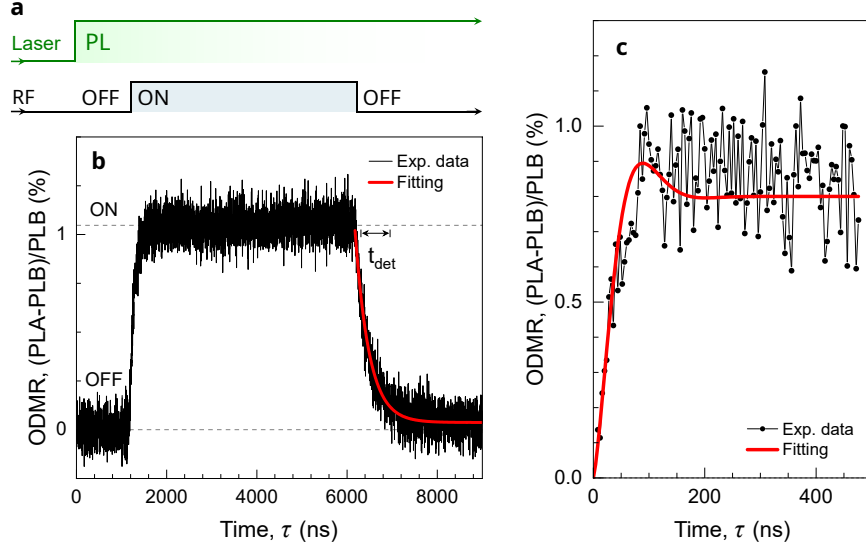


Fig. S3: (a) Pulse sequence used to measure the relative change in the PL intensity ( $\Delta PL/PL$ ) upon switching the RF field on and off. (b) RF-induced transient change  $C = \Delta PL/PL$  in sample #1 at  $T = 10$  K. The thick red line represents a mono-exponential fit of the PL decrease after the RF field is switched off. The red thick line represents a mono-exponential fit to the PL decay after the RF field is switched off. This fit defines the detection window  $t_{det}$  used to measure  $PL_A$  and  $PL_B$ , as described in the main text. (c) Rabi measurement performed using the protocol described in the main text. The red thick line shows a fit to the function  $C(\tau) = C_\infty (1 - \cos \omega_R \tau) e^{-(\frac{\tau}{T_R})^k}$  with  $C = 0.8 \pm 0.1$ ,  $\omega_R/2\pi = 4.3 \pm 0.4$  MHz,  $T_R = 50 \pm 10$  ns and  $k = 1.2 \pm 0.3$ .

### Supplementary Figure S4: Ramsey fringes

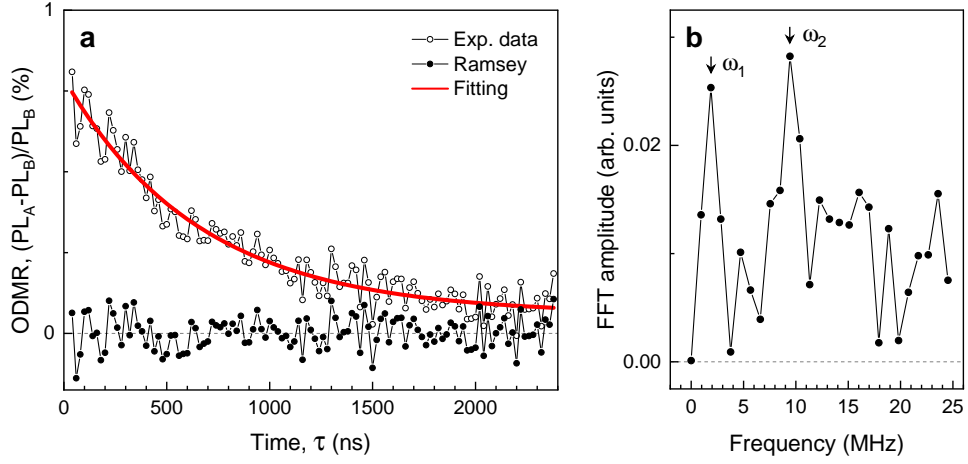


Fig. S4: (a) Open symbols represent experimental data obtained from sample #1 at  $T = 10$  K using the protocol for measuring  $T_2^*$ , as described in the main text. The red thick line shows a fit with a fixed exponential decay time determined from the  $T_1$  measurement. Closed symbols represent the experimental data after subtraction of the exponential decay associated with quenching of the ODMR contrast. (b) Fast Fourier transform (FFT) of the experimental data after subtraction of the exponential decay. The vertical arrows indicate the frequencies of the Ramsey oscillations  $\omega_1$  and  $\omega_2$  used to fit the data in the main text.

## Supplementary Figure S5: Experimental geometry

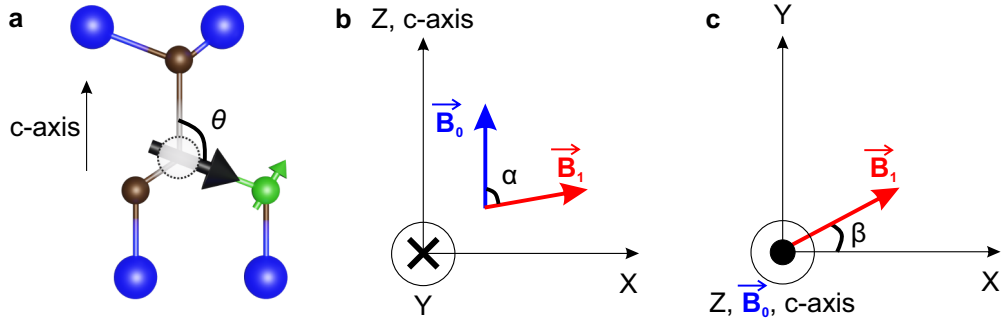


Fig. S5: (a) The 4H-SiC crystal c-axis is oriented along the  $Z$  axis of the laboratory coordinate system. Angle  $\theta$  is defined as the tetrahedral angle. (b) The external magnetic field  $\vec{B}_0 \parallel Z$  is oriented along the c-axis. The driving RF field  $\vec{B}_1$  is oriented at angle  $\alpha$  with respect to the  $Z$  axis in the  $ZX$  plane. (c) The RF driving field  $\vec{B}_1$  is oriented at angle  $\beta$  with respect to the  $X$  axis in the  $XY$  plane.

## SUPPLEMENTARY TEXT

### Supplementary Text S1: Simulation of the ODMR spectra

This code provides a quantitative simulation of ODMR spectrum of a spin defect in a crystalline environment, incorporating zero-field splitting, hyperfine interaction, external magnetic field and orientation effects. The code was run on MATLAB 2022b with package EasySpin 6.0.

0. Reset the work space:

```
clear; %Removes all previously defined variables
clf; %Clears the current figure window
```

1. Define the spin system:

```
S = 1; %Electron spin
I = 3/2; %Nuclear spin
SiC_Cl.S = [1]; %Definition of spin system
SiC_Cl.g = [2.0028]; %Electron g factor
SiC_Cl.D = [560 60]; %Zero-field splitting parameters [D E] in MHz
SiC_Cl.Nucs = ['35Cl']; %Definition of nuclear spin
SiC_Cl.A = -34; %Hyperfine coupling constant in MHz
SiC_Cl.lwpp = 15; %Peak-to-peak linewidth in MHz
```

2. Define the initial spin state due to optical pumping, i.e., only the  $m_s = \pm 1$  spin states are assumed to be equally populated, while the population of the  $m_s = 0$  spin states is zero:

```
Sz = sop([S I], 'z1'); %Electronic spin projection on z
rho = abs(Sz)/8; %Density matrix rho 12 by 12
SiC_Cl.initState = {rho, 'uncoupled'}; %Set initial spin state
```

3. Experiment parameters

3.1. Define crystal symmetry

```
Exp.CrystalSymmetry = 'Cs'; %Set the point group
Exp.Frame = 'crystal'; %Sample in the crystal coordinate system
```

3.2. Define static magnetic field

```
Exp.Field = 6.7 %Magnetic field in mT along z
```

3.3. Define RF driving field, with the propagation direction and polarization angle  $\alpha$  ( $\alpha$ ) of the RF field explained in Fig. S5:

```
mwRange = [0 1] %RF range in GHz
Exp.mwRange = mwRange;
Exp.Harmonic = 0; %Only fundamental harmonic
alpha = 80*pi/180; %Polarization angle
Exp.mwMode = {'y', alpha}; %RF propagation and polarization
```

3.4. Define orientation of the lab frame, with the Euler angles  $\beta$  ( $\beta$ ) and  $\theta$  ( $\theta$ ) for the lab frame to the sample frame transformation explained in Fig. S5:

```
beta = deg2rad(28); %Orientation of RF wire
theta = deg2rad(acosd(-(1/3))); %Tetrahedral angle
Exp.SampleFrame = [beta theta 0]; %Set Euler angles
```

4. Define output arguments and simulation options:

```
Opt.Threshold = 1e-1; %Remove weak transitions
Opt.Verbosity = 2; %Diagnostic output
```

5. Perform simulation and plot spectra:

```
[nu, spec, info] = pepper(SiC_Cl, Exp, Opt); %Call main function
plot(nu, abs(spec), 'r'); %Plot spectrum
```

## SUPPLEMENTARY TABLES

### Supplementary Table S1: Spin state decomposition

TABLE S1: The decomposition is performed in the basis  $|m_S, m_I\rangle$  for  $B = 0$  mT. The energies are given in MHz relative to the minimum energy.

Level	Energy	$ -1, -3/2\rangle$	$ -1, -1/2\rangle$	$ -1, 1/2\rangle$	$ -1, 3/2\rangle$	$ 0, -3/2\rangle$	$ 0, -1/2\rangle$	$ 0, 1/2\rangle$	$ 0, 3/2\rangle$	$ 1, -3/2\rangle$	$ 1, -1/2\rangle$	$ 1, 1/2\rangle$	$ 1, 3/2\rangle$
1	0	0	0	0	0	0.01	0	0.98	0	0	0.01	0	0
2	0	0	0	0.01	0	0	0.98	0	0.01	0	0	0	0
3	4	0	0	0	0	0	0.01	0	0.98	0	0	0.01	0
4	4	0	0.01	0	0	0.98	0	0.01	0	0	0	0	0
5	489	0	0	0	0.17	0	0	0	0	0	0	0	0.83
6	489	0.83	0	0	0	0	0	0	0	0.17	0	0	0
7	508	0	0.63	0	0	0	0	0	0	0	0.36	0	0
8	508	0	0	0.36	0	0	0	0	0	0	0	0.63	0
9	632	0	0.35	0	0.02	0	0	0	0	0	0.62	0	0
10	632	0	0	0.62	0	0	0	0	0	0.02	0	0.35	0
11	648	0	0.01	0	0.81	0	0	0	0	0	0.01	0	0.17
12	648	0.17	0	0.01	0	0	0	0	0	0.81	0	0.01	0